NACA TN 3036

NATIONAL ADVISORY COMMITTEE FOR AERONAUTICS

TECHNICAL NOTE 3036

THE FLOW ABOUT A SECTION OF A FINITE-

ASPECT-RATIO NACA 0018 AIRFOIL

ON A TRANSONIC BUMP

By Jack A. Mellenthin

Ames Aeronautical Laboratory
Moffett Field, Calif.

NACA

Washington

October 1953

NATIONAL ADVISORY COMMITTEE FOR AERONAUTICS

TECHNICAL NOTE 3036

THE FLOW ABOUT A SECTION OF A FINITE-

ASPECT-RATIO NACA 0015 AIRFOIL

ON A TRANSONIC BUMP

By Jack A. Mellenthin

SUMMARY

Pressure distributions on a semispan rectangular wing model having an NACA 0015 airfoil section and a moderate aspect ratio were measured at one spanwise station in tests made on a transonic bump in the Ames 16-foot high-speed wind tunnel. The free-stream Mach number range was from 0.4 to 1.06. The results showed that at a fixed angle of attack a region developed over the airfoil wherein the Mach number at each point remained essentially constant as the free-stream Mach number was increased above the critical. This region covered essentially the whole chord of the airfoil at free-stream Mach numbers near unity.

INTRODUCTION

An understanding of the adverse aerodynamic characteristics experienced by airfoils in the transonic region is dependent upon a comprehension of the flow changes which cause such characteristics. Toward this end, considerable work has been done in the study of the nature of transonic flow. Of special interest are the investigations reported in references 1 to 5. In these references it has been recognized that at transonic Mach numbers a region exists on the surface of an airfoil wherein, at a fixed angle of attack, the local Mach number remains essentially constant with increasing free-stream Mach number. The present investigation supplies additional information on the characteristics of this constant local Mach number region through the range of transonic free-stream Mach numbers up to 1.06 where data have heretofore been rather meager.

The results of the present investigation do not correspond strictly to two-dimensional flow since a finite-span model having a moderate aspect ratio was used. Chordwise distribution of surface pressures

were measured at only one station. To reduce the effect of aspect ratio
on the data, this orifice station was located far inboard from the
model tip.

NOTATION

a   local speed of sound, ft/sec

c   airfoil chord, ft

c_{d_p} section pressure drag coefficient, $\dfrac{\text{section pressure drag}}{qc}$

c_l section lift coefficient, $\dfrac{\text{section lift}}{qc}$

c_m section pitching-moment coefficient, about the quarter-chord

       point, $\dfrac{\text{section pitching moment}}{qc^2}$

M   average free-stream Mach number, $\dfrac{V}{a}$

M_l local Mach number, $\dfrac{V_l}{a}$

P   pressure coefficient, $\dfrac{p_l - p}{q}$

P_{cr} pressure coefficient at which local sonic velocity occurs

p_l local static pressure, lb/sq ft

p   free-stream static pressure, lb/sq ft

q   free-stream dynamic pressure, lb/sq ft

R   Reynolds number

V   free-stream airspeed, ft/sec

V_l local airspeed, ft/sec

x   chordwise distance behind the leading edge of the airfoil, ft

y   airfoil ordinate, ft

α geometrical angle of attack, deg

APPARATUS AND TESTS

A semispan wing model mounted on a transonic bump in the Ames 16-foot wind tunnel was used in the present investigation (figs. 1 and 2). This model had the NACA 0015 section, a 6-inch chord, a semispan of approximately 12 inches, an aspect ratio of about 4, and was the same model used in the two-dimensional investigations reported in references 1 and 2. For the present tests, the model was modified by adding a tip fairing and by putting orifices on both the upper and lower surfaces at 0.25-percent and 1.25-percent chord, so that additional data could be obtained near the leading edge. (See table I.) To decrease the effects of the bump boundary layer on the flow over the wing, a fence was installed on the airfoil 3/4 inch from the bump surface. A wooden fairing was included between this fence and the bump surface to house the model support bracket. The model and wooden fairing (figs. 1 and 2) were mounted on a turntable flush with the bump contour, and the angle of attack was changed by rotating this turntable. The effect of the wooden fairing on the data is believed to be small.

The row of pressure orifices on the model was 2 inches from the fence. Pressures were measured on the upper and lower surfaces of the airfoil using a mercury-in-glass, multiple manometer.

During this investigation, only pressures on the upper and lower surfaces of the model were measured. The force and moment data were obtained by mechanical integration of the pressure-distribution plots. The pressures were measured through an angle-of-attack range from -4° to $+15^\circ$, and the Mach number range was from 0.4 to 1.06, while the corresponding Reynolds number range (fig. 3) was from approximately 1.3 million to 2.1 million. The dynamic pressure in the test region was held within 0.5 percent of its predetermined values, and the angle-of-attack measuring device was accurate within $\pm 0.1^\circ$.

Mach number contours over the bump in the absence of the model are shown in figure 4. The heavy dashed lines in this figure indicate the model location. The reference free-stream Mach numbers shown are averages of the local Mach numbers over the orifice station.

RESULTS AND DISCUSSION

Pressure Measurements

Representative chordwise pressure distributions for angles of attack of 0.5°, 4°, and 8° are shown in figures 5 to 7. (The test results showed that the section lift was equal to zero at an angle of attack of about 0.5°.) Values of the critical pressure coefficient are shown in

the figures for free-stream Mach numbers below 1.00 where mixed flow was present.

The changes which took place in the distributions of pressure as the free-stream Mach number increased through unity are quite apparent in these figures. At angles of attack of 4° and 8° it is evident, as indicated by the locations of abrupt increases in the pressure coefficient at low supercritical Mach numbers, that the shock wave on the lower surface moved downstream rapidly as the free-stream Mach number was increased, while the shock wave on the upper surface moved downstream much less rapidly. Consequently, over the rearward portion of the airfoil, greater negative pressures occurred on the lower surface than on the upper surface. This sequence of events produced a reduced, or in some cases a negative, lift on the airfoil, as will be discussed later in this report. As the free-stream Mach number was increased further, the shock wave on each surface moved downstream to the trailing edge, eliminating the region of negative lift. The accompanying recovery of the lift will also be discussed later.

Region of Nearly Constant Local Mach Number

Local Mach numbers over the airfoil surface for angles of attack of 0.5°, 4°, and 8° have been determined from the pressure coefficients of the present investigation, using isentropic relations, and are presented at selected chordwise stations in figures 8 to 10 as a function of free-stream Mach number. As the test Mach number was increased above the critical, a small region developed over the forward part of the airfoil at an angle of attack of 0.5° (fig. 8) wherein the Mach number at each point remained essentially constant with increasing free-stream Mach number. For example, at 5-percent chord the local Mach number increased only about 0.02 while the free-stream Mach number was increased about 0.20 (from 0.85 to 1.05). At angles of attack of 4° and 8°, the region of constant local Mach number formed first at low supercritical Mach numbers at about the 5-percent-chord station on the upper surface, and, as the Mach number was increased further, this region spread both forward and rearward on the upper surface, reaching the leading edge, and becoming established on the forward portion of the lower surface at a free-stream Mach number of about 0.9. At all three angles of attack (figs. 8 to 10), the region essentially covered the airfoil from the leading edge to the trailing edge at a free-stream Mach number of unity.

It is also observed in figures 8 to 10 that, as the free-stream Mach number was increased, the local Mach number for rearward chordwise stations increased rapidly before the relatively constant region was formed. On the upper surface, at angles of attack of 4° and 8°, this increase was more gradual than at an angle of attack of 0.5° (figs. 9(a) and 10(a)).

Force and Moment Characteristics

The force and moment characteristics, which were obtained by mechanical integration of the pressure-distribution plots, are presented in figure 11. From this figure, it may be seen that the airfoil exhibited undesirable variations of section lift, pressure-drag, and pitching-moment coefficients at the high subsonic Mach numbers.

The adverse variations of lift and pitching moment resulted from the previously discussed rearrangement of pressures on the upper and lower airfoil surfaces at high subsonic Mach numbers. Most of the lift reduction took place between free-stream Mach numbers of 0.75 and 0.85 and was so severe at a Mach number of 0.88 that the section lift coefficient actually was negative at a positive angle of attack of 4°. As a Mach number of unity was approached, the lift recovered somewhat, as may be seen in figure 11. This recovery, which resulted from the previously mentioned behavior of the pressures, occurred principally between free-stream Mach numbers of 0.90 and 0.96. The unusually large variations of the pitching-moment coefficients at high subsonic Mach numbers, shown in figure 11 near 0 angle of attack, indicate correspondingly large variations in the chordwise center-of-pressure location in this Mach number range. The amount of pressure drag contributed by the parts of the airfoil forward and rearward of the point of maximum thickness has been determined at an angle of attack of 0.5° and is presented in figure 12 together with the total pressure drag for comparison. The initial total pressure drag rise with increasing transonic free-stream Mach number resulted principally from decreasing pressure coefficients over the rear part of the airfoil. However, at Mach numbers near 1 an increasing part of the total pressure drag was due to the increasing pressures over the forward part of the airfoil.

CONCLUDING REMARKS

As the free-stream Mach number was increased above the critical, a region of nearly constant local Mach number formed near the leading edge of the airfoil at zero lift. At higher angles of attack, this region formed first at about the 5-percent-chord station on the upper surface at low supercritical Mach numbers. The region spread both forward and rearward as the free-stream Mach number was increased, reaching the leading edge and becoming established on the forward portion of the lower surface at a free-stream Mach number of about 0.90. When the Mach number of the free stream was increased further, the region of nearly constant Mach number expanded rearward for each angle of attack

until essentially the entire chord of the airfoil was included at a
free-stream Mach number of unity.

Ames Aeronautical Laboratory
    National Advisory Committee for Aeronautics
        Moffett Field, Calif., Aug. 27, 1953

REFERENCES

1. Graham, Donald J., Nitzberg, Gerald E., and Olson, Robert N.:
    A Systematic Investigation of Pressure Distributions at High
    Speeds Over Five Representative NACA Low-Drag and Conventional
    Airfoil Sections. NACA Rep. 832, 1945.

2. Nitzberg, Gerald E., and Crandall, Stewart: A Study of Flow Changes
    Associated with Airfoil Section Drag Rise at Supercritical Speeds.
    NACA TN 1813, 1949.

3. Bryson, Arthur Earl, Jr.: An Experimental Investigation of Transonic
    Flow Past Two-Dimensional Wedge and Circular-Arc Sections Using
    a Mach-Zehnder Interferometer. NACA TN 2560, 1951.

4. Tsien, Hsue-Shen, and Fejer, Andrej: A Method for Predicting the
    Transonic Flow Over Airfoils and Similar Bodies from Data Obtained
    at Small Mach Numbers. GALCIT, 1944.

5. Gullstrand, Tore R.: A Theoretical Discussion of Some Properties
    of Transonic Flow over Two-Dimensional Symmetrical Aerofoils at
    Zero Lift with a Simple Method to Estimate the Flow Properties.
    KTH Aero TN 25, 1952, Royal Inst. of Tech., Stockholm, Sweden.

TABLE I.- MODEL COORDINATES AND PRESSURE-ORIFICE STATIONS

[Stations and ordinates in percent of airfoil chord]

NACA 0015 coordinates		Pressure-orifice stations	
Station	Ordinate	Upper surface	Lower surface
0	0	0	0
1.250	2.367	.250	.250
2.500	3.268	1.250	1.250
5.000	4.443	2.500	2.500
7.500	5.250	5.000	5.000
10.000	5.853	10.000	10.000
15.000	6.681	15.000	15.000
20.000	7.172	20.000	20.000
25.000	7.427	25.000	25.000
30.000	7.502	30.000	30.000
40.000	7.254	35.000	35.000
50.000	6.618	40.000	40.000
60.000	5.704	45.000	45.000
70.000	4.580	50.000	50.000
80.000	3.279	55.000	55.000
90.000	1.810	60.000	60.000
95.000	1.008	70.000	70.000
100.000	(.158)	80.000	80.000
100.000	0	87.500	90.000
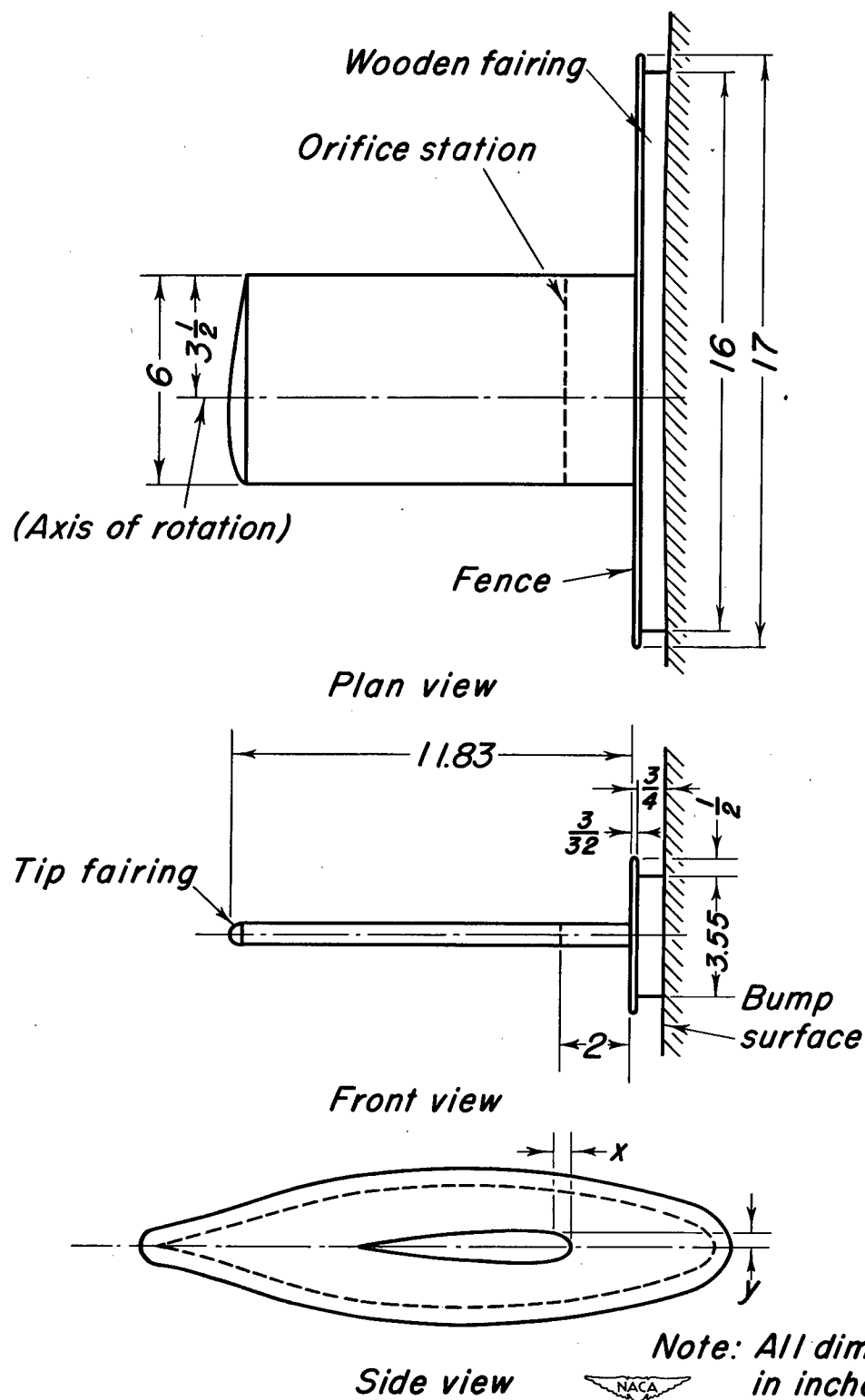
Figure 1.- Three-view drawing of the model on the transonic bump of the Ames 16-foot wind tunnel.
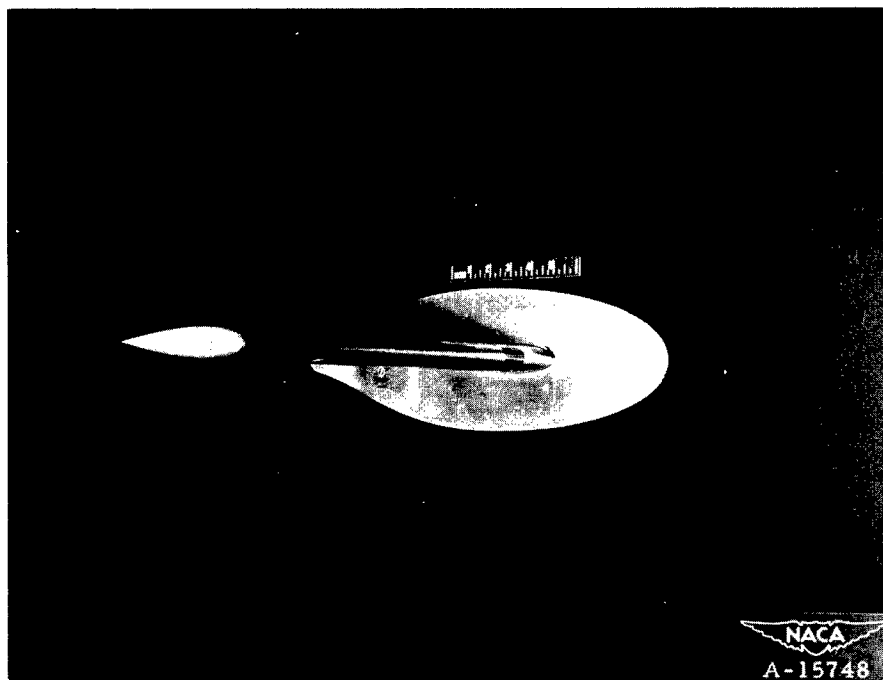
(a) Three-quarter front view.
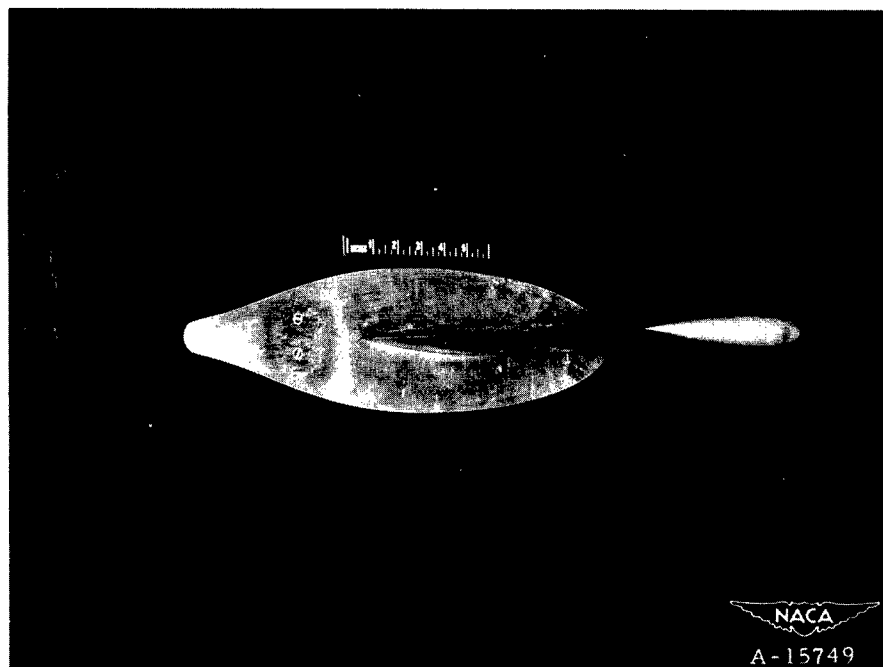
(b) Three-quarter rear view.

Figure 2.- The model on the transonic bump of the Ames 16-foot wind tunnel.
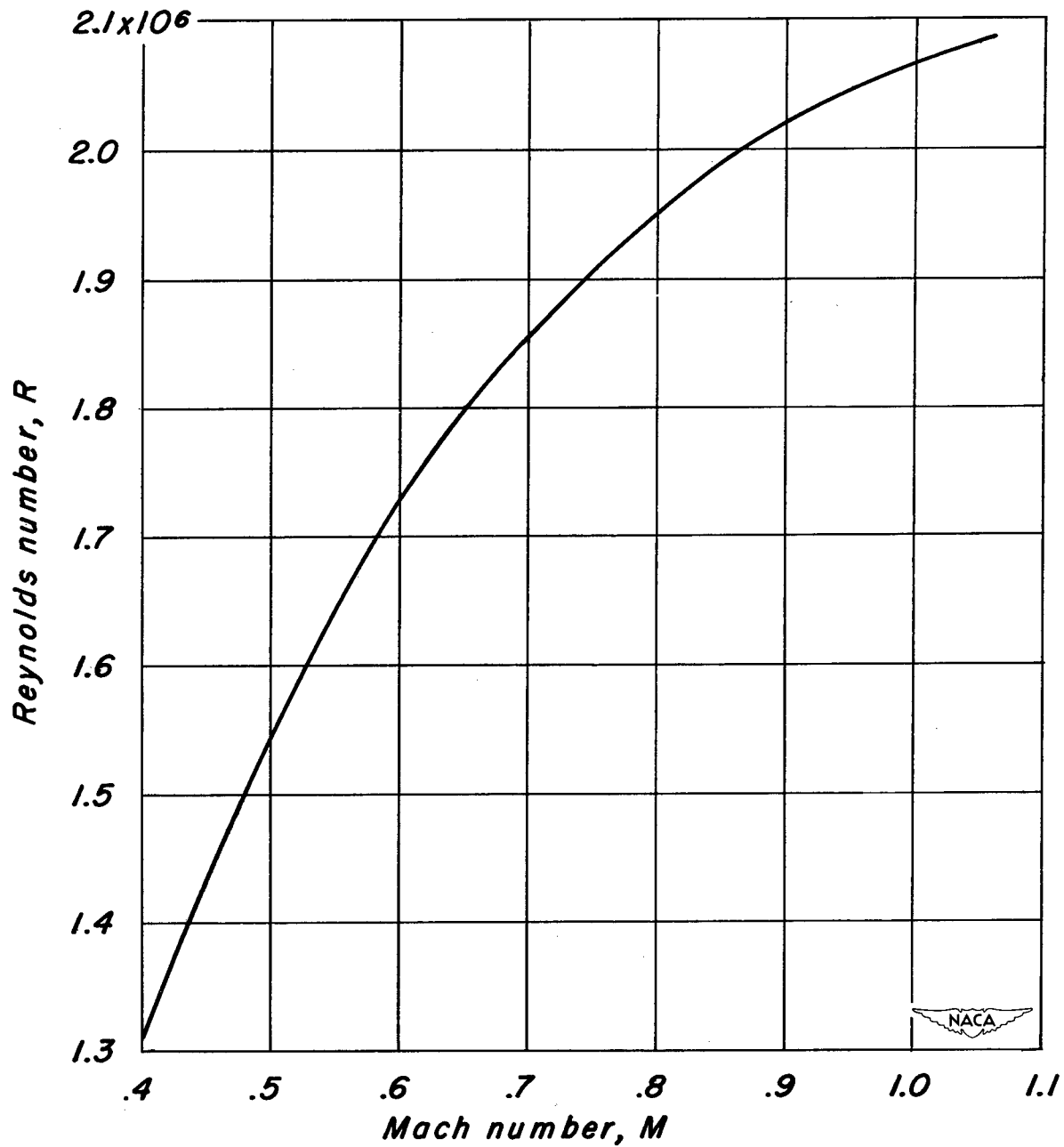
Figure 3.- Variation of Reynolds number with Mach number during the
16-foot wind-tunnel test of the NACA 0015 airfoil model.
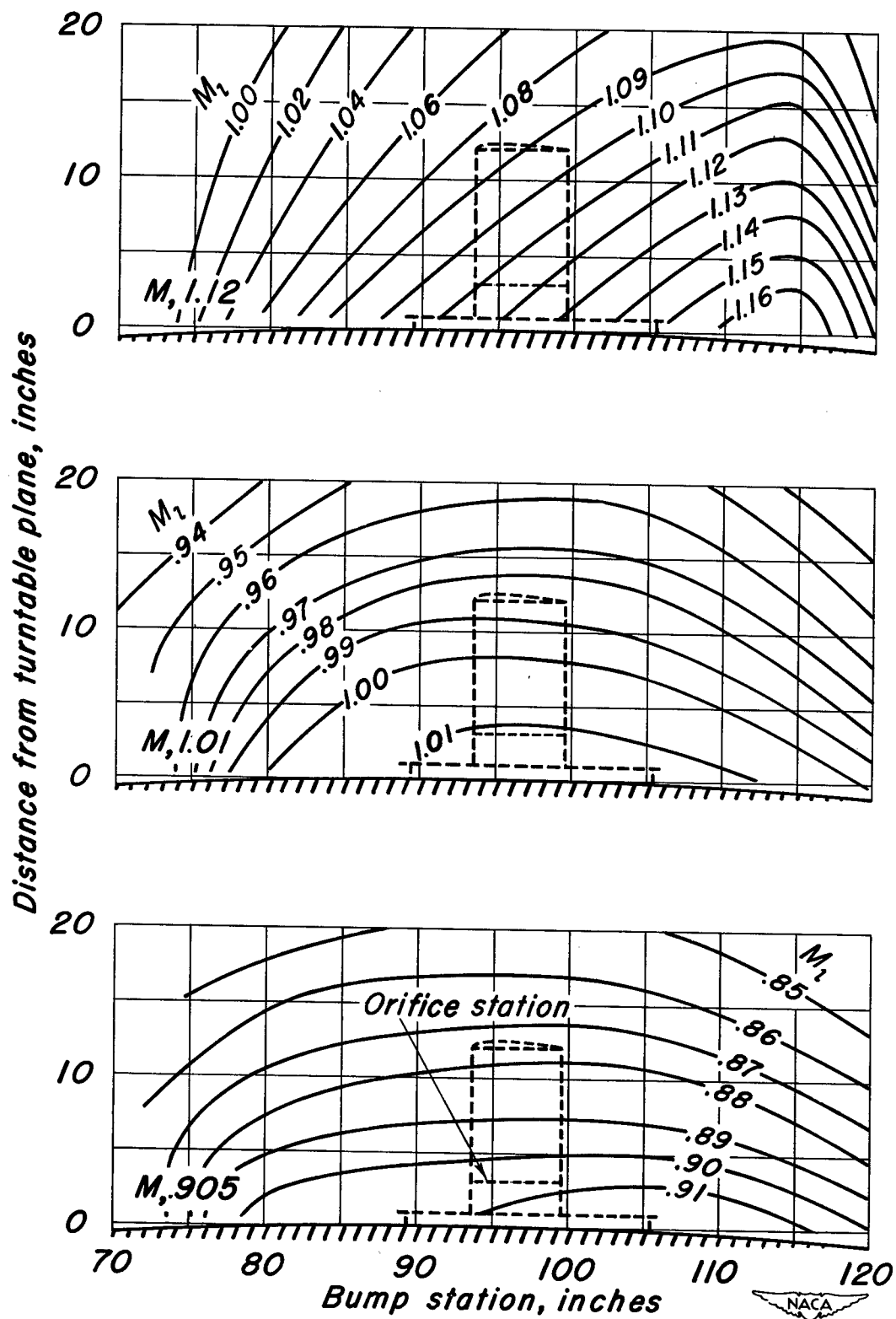
Figure 4.- Typical Mach number contours over the Ames 16-foot tunnel transonic bump.
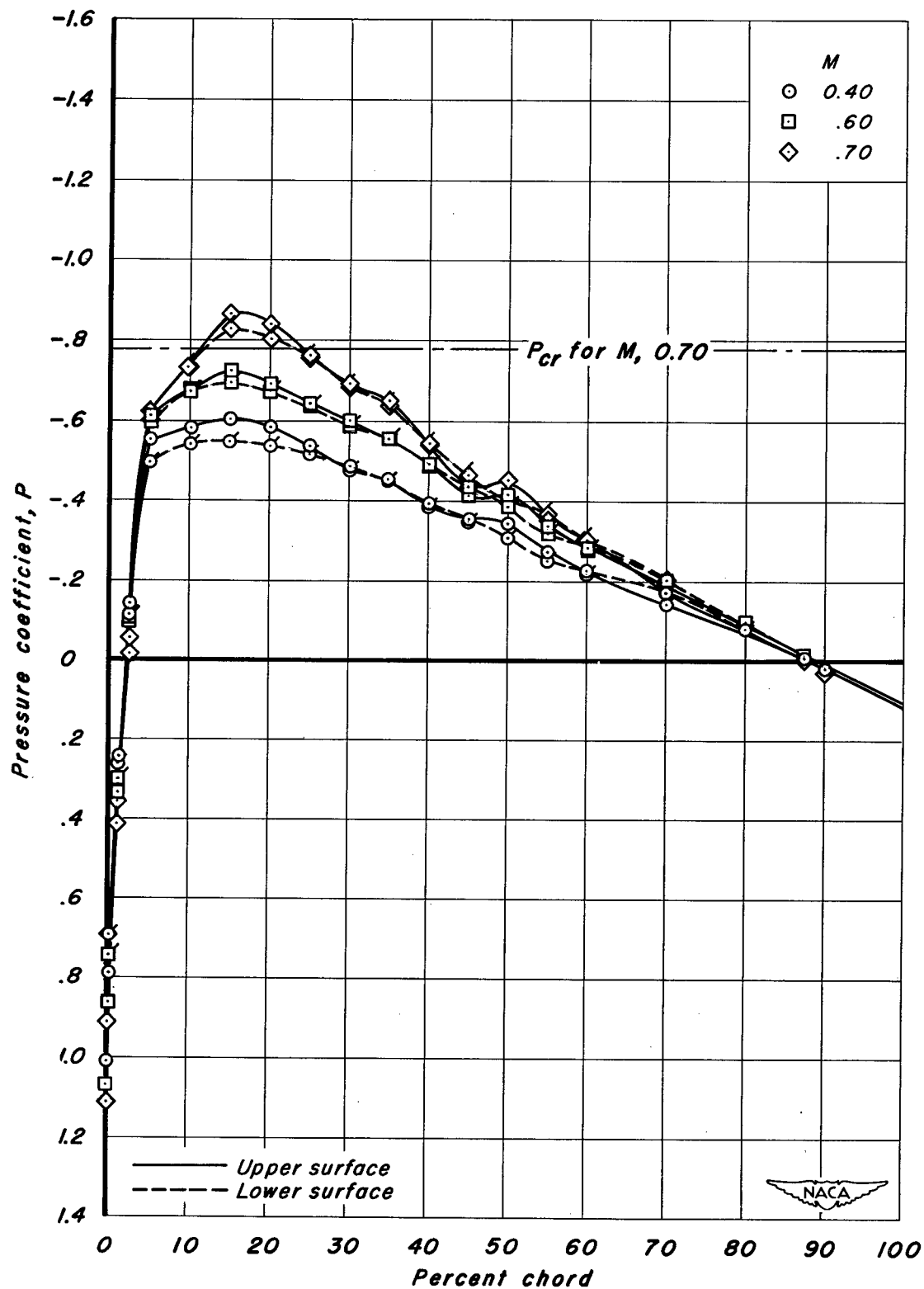
(a) M, 0.40, 0.60, and 0.70

Figure 5.- Effect of Mach number on the chordwise distribution of
pressure coefficient, $\alpha = 0.5^\circ$ (approximately zero lift).
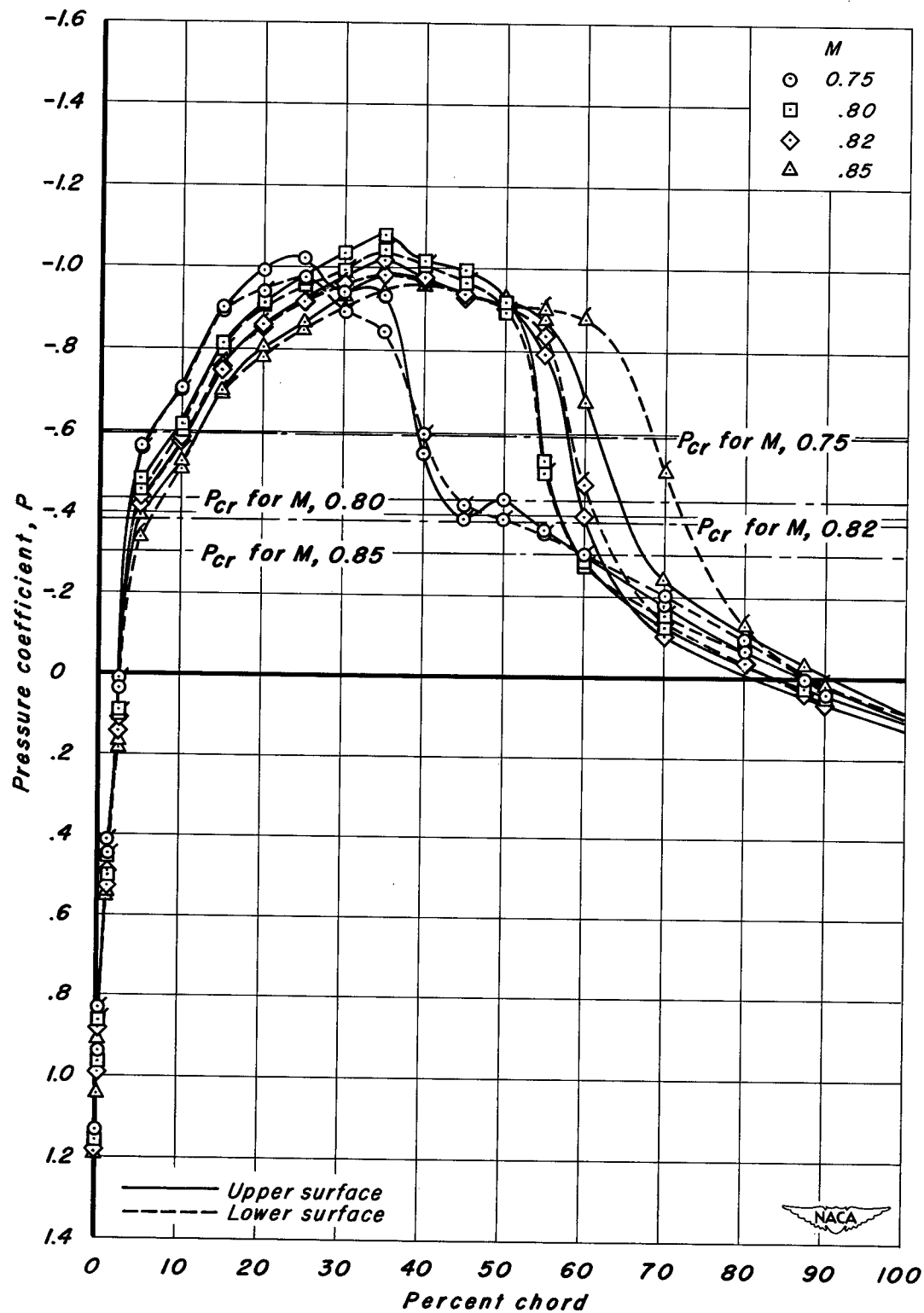
(b) M, 0.75, 0.80, 0.82, and 0.85

Figure 5.- Continued.
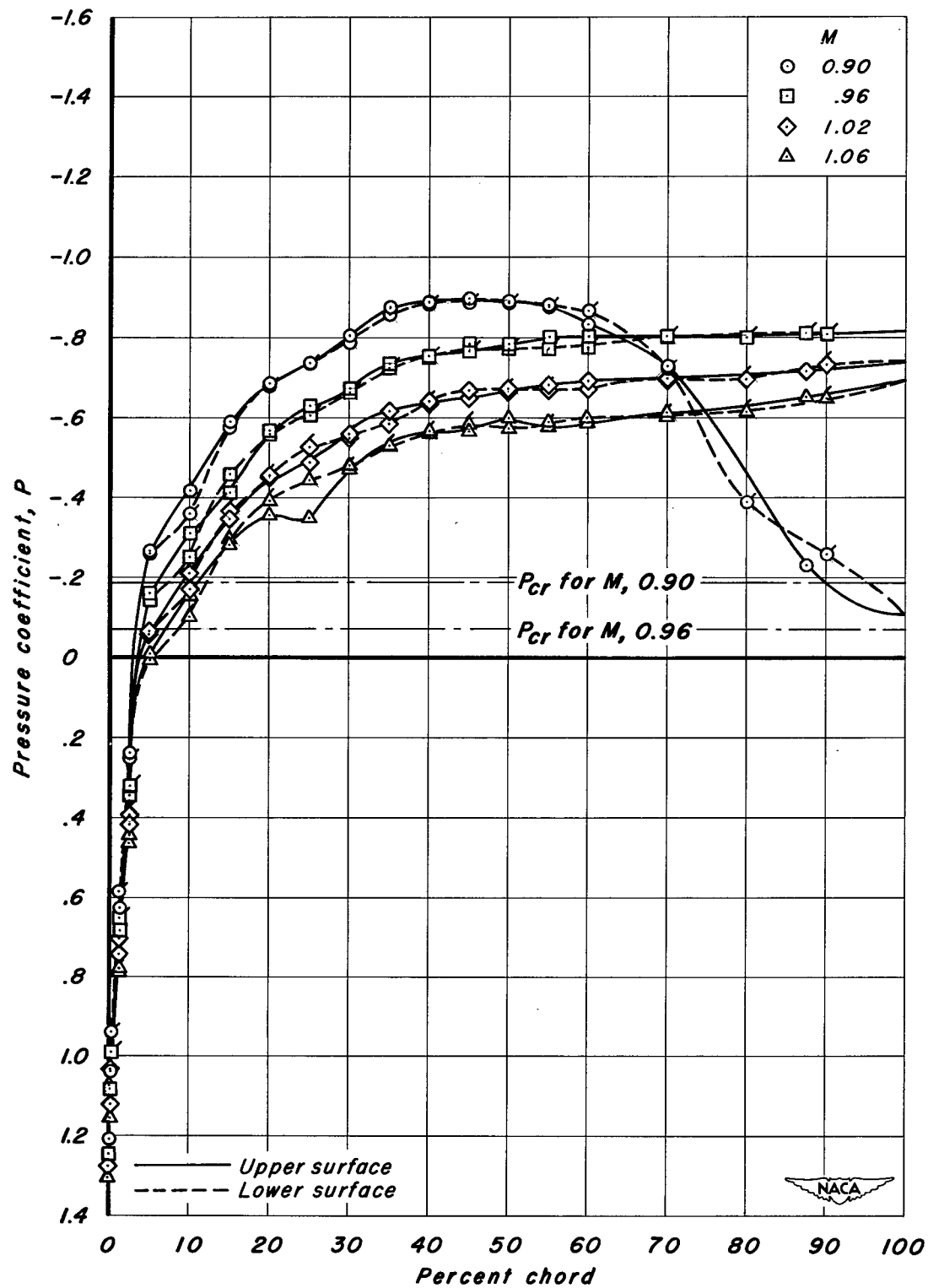
(c) M, 0.90, 0.96, 1.02, and 1.06

Figure 5.- Concluded.
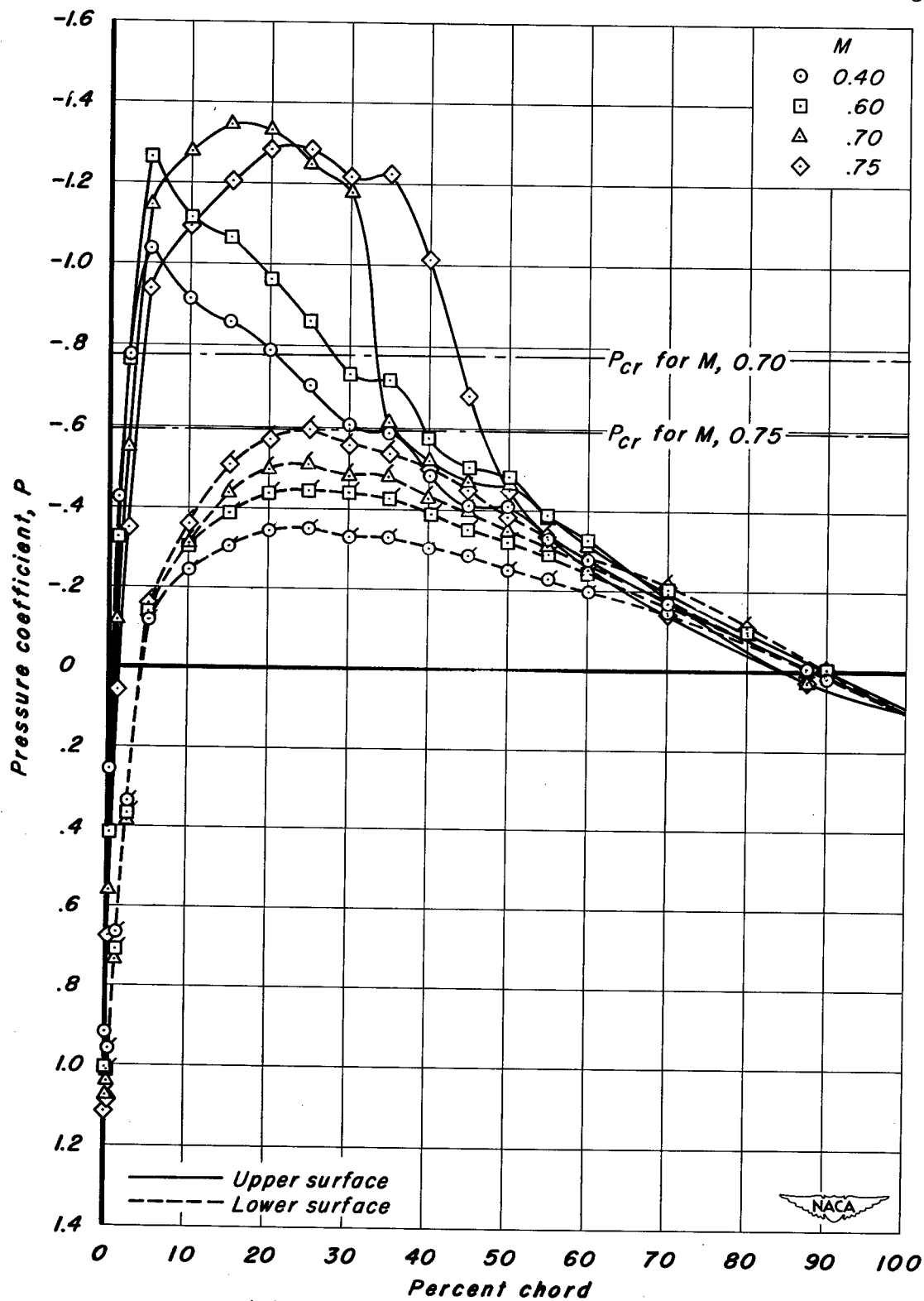
(a) M, 0.40, 0.60, 0.70, and 0.75

Figure 6.- Effect of Mach number on the chordwise distribution of pressure coefficient, $\alpha = 4.0^{\circ}$.
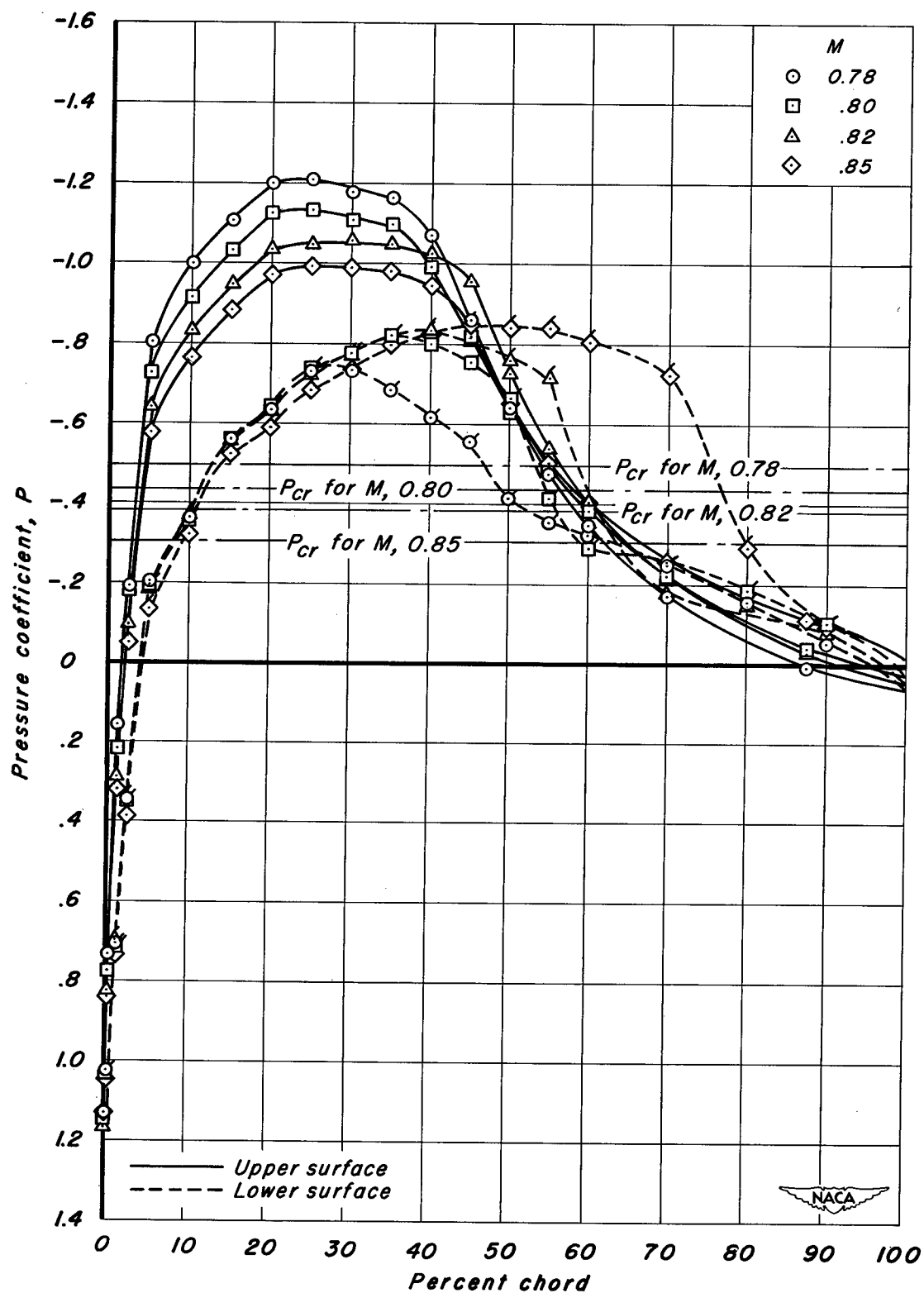
(b) M, 0.78, 0.80, 0.82, and 0.85

Figure 6.- Continued.
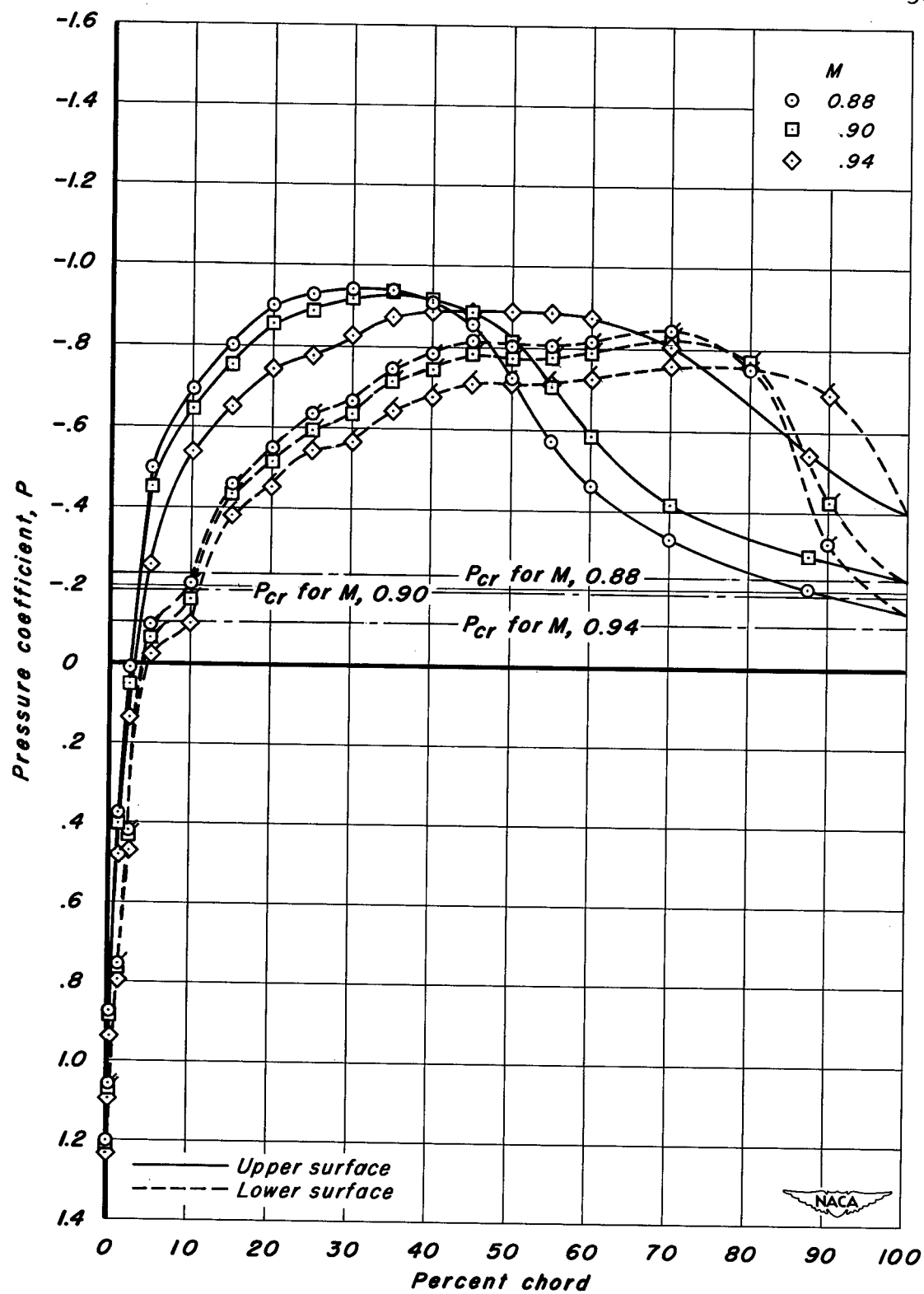
(c) M, 0.88, 0.90, and 0.94

Figure 6.- Continued.
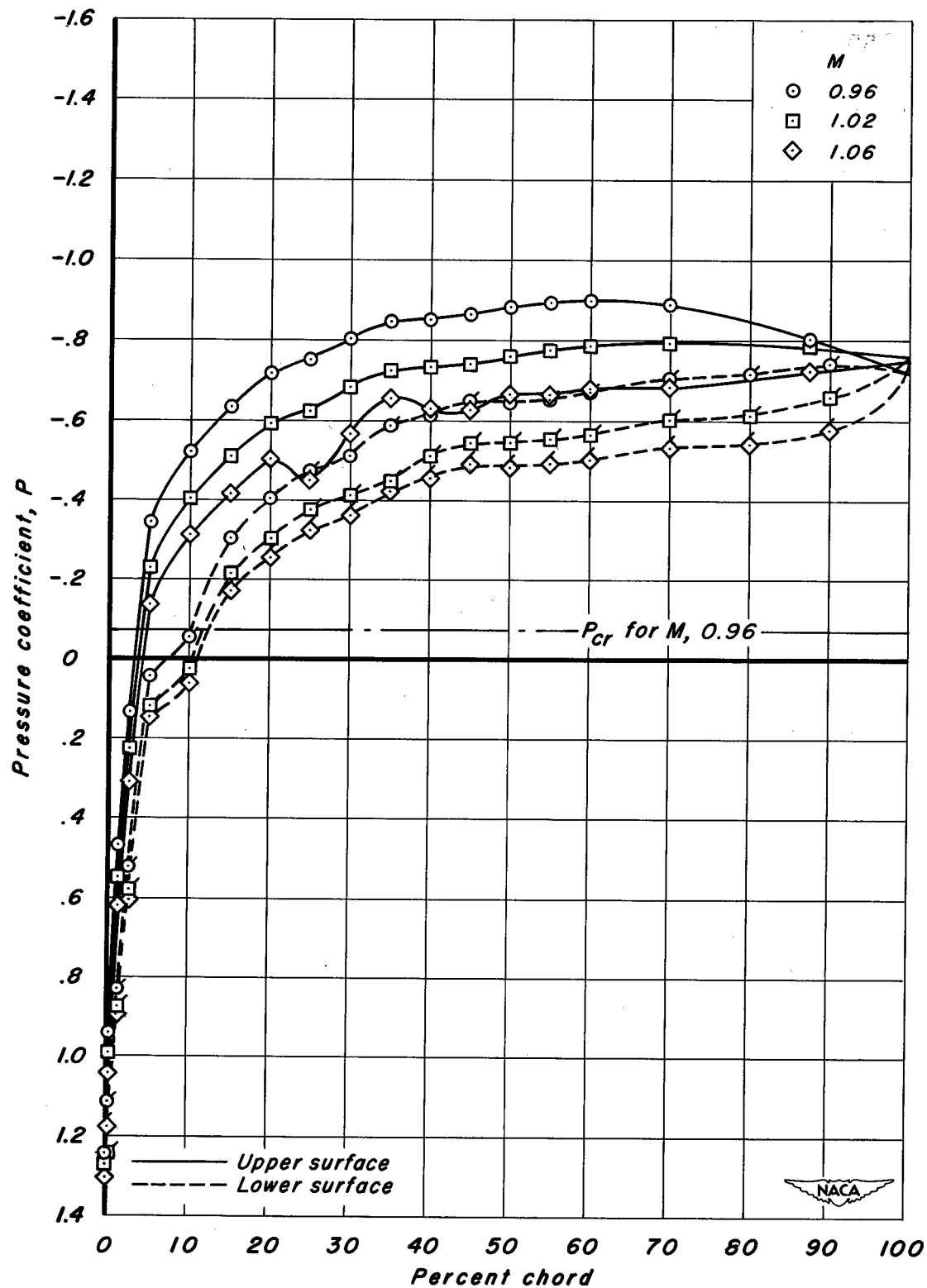
(d) M, 0.96, 1.02, and 1.06

Figure 6.- Concluded.
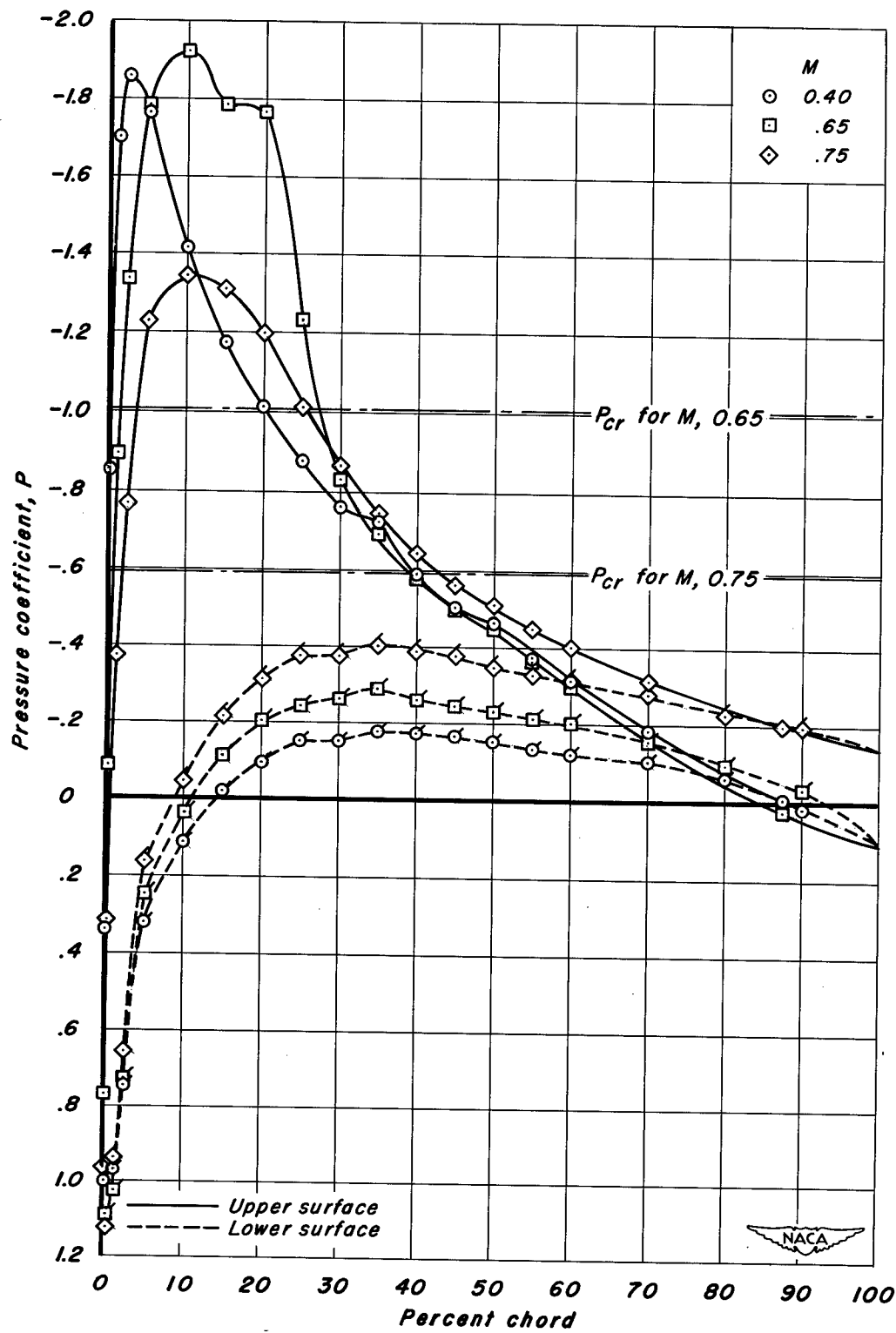
(a) M, 0.40, 0.65, and 0.75

Figure 7.- Effect of Mach number on the chordwise distribution of pressure coefficient, $\alpha = 8.0^\circ$.
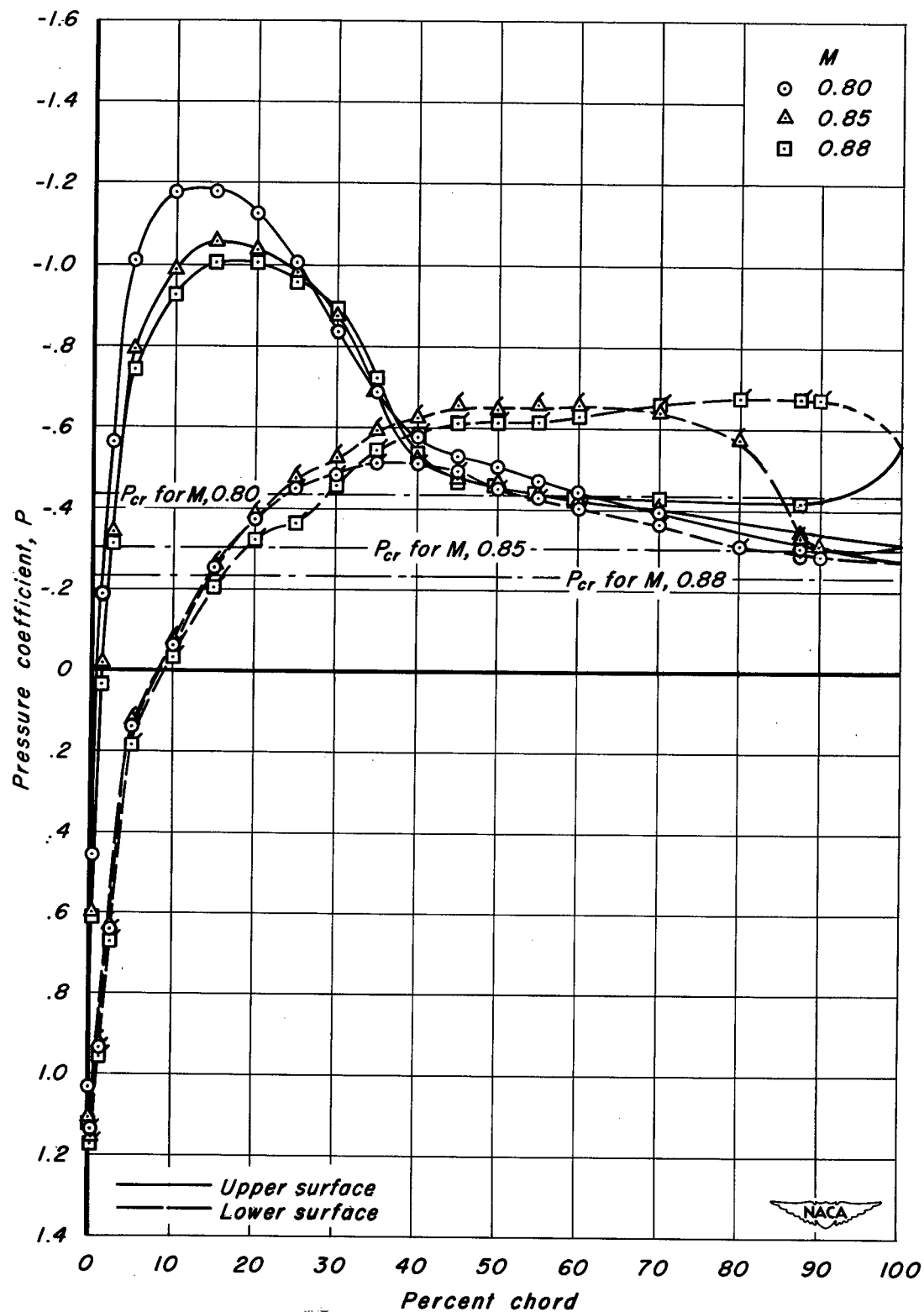
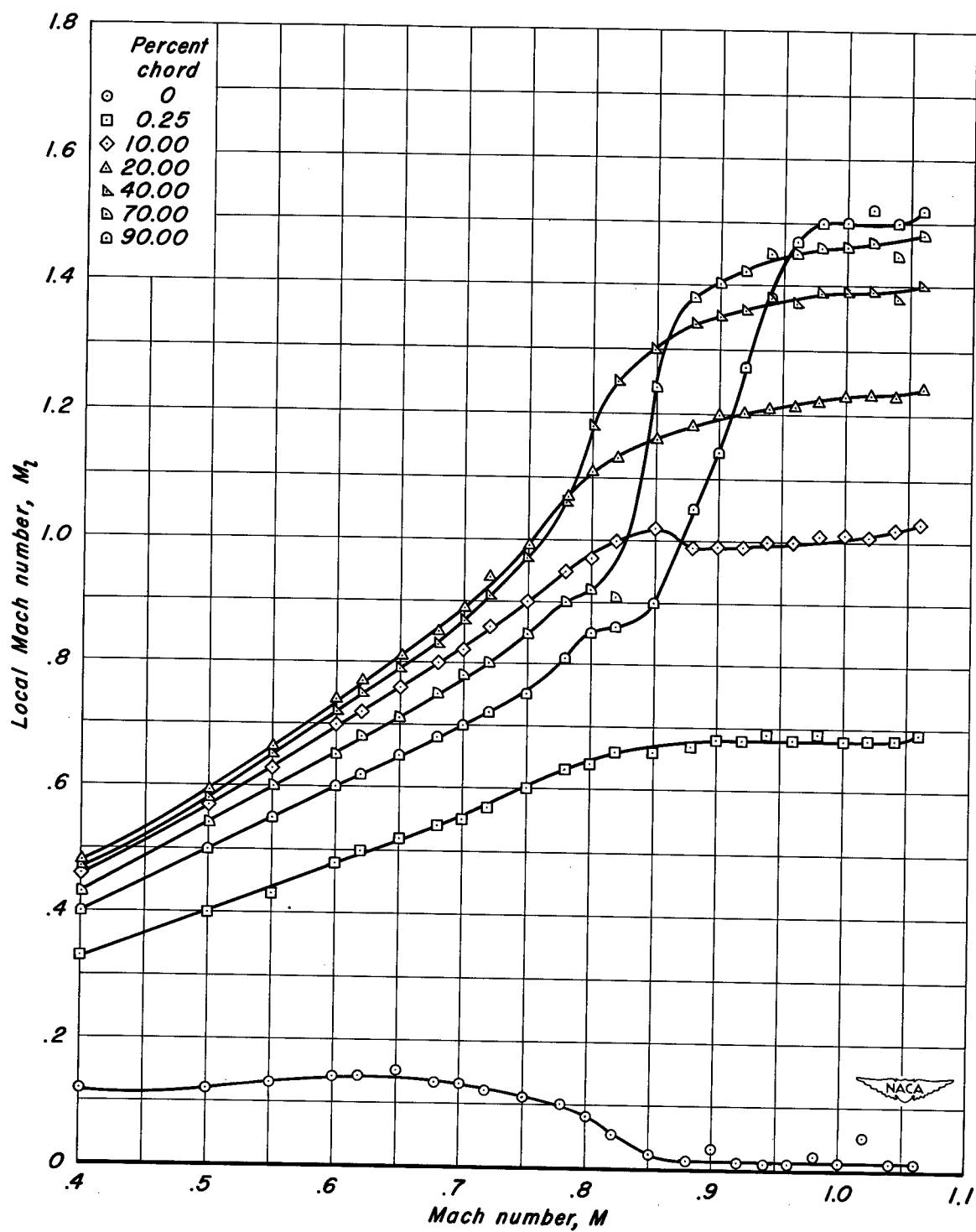(b) M, 0.80, 0.85, and 0.88

Figure 7.- Continued.
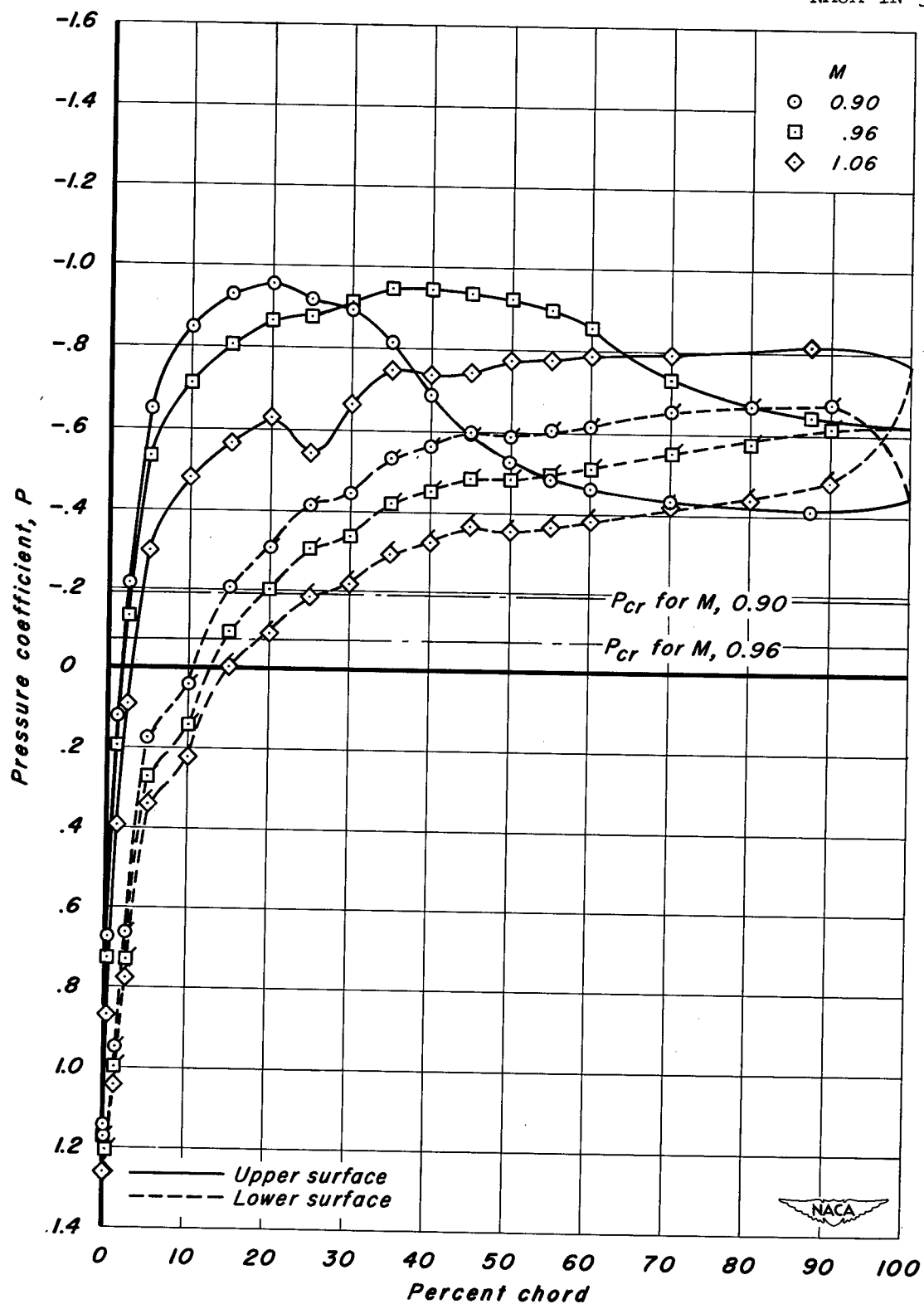
(c) M, 0.90, 0.96, and 1.06

Figure 7.- Concluded.
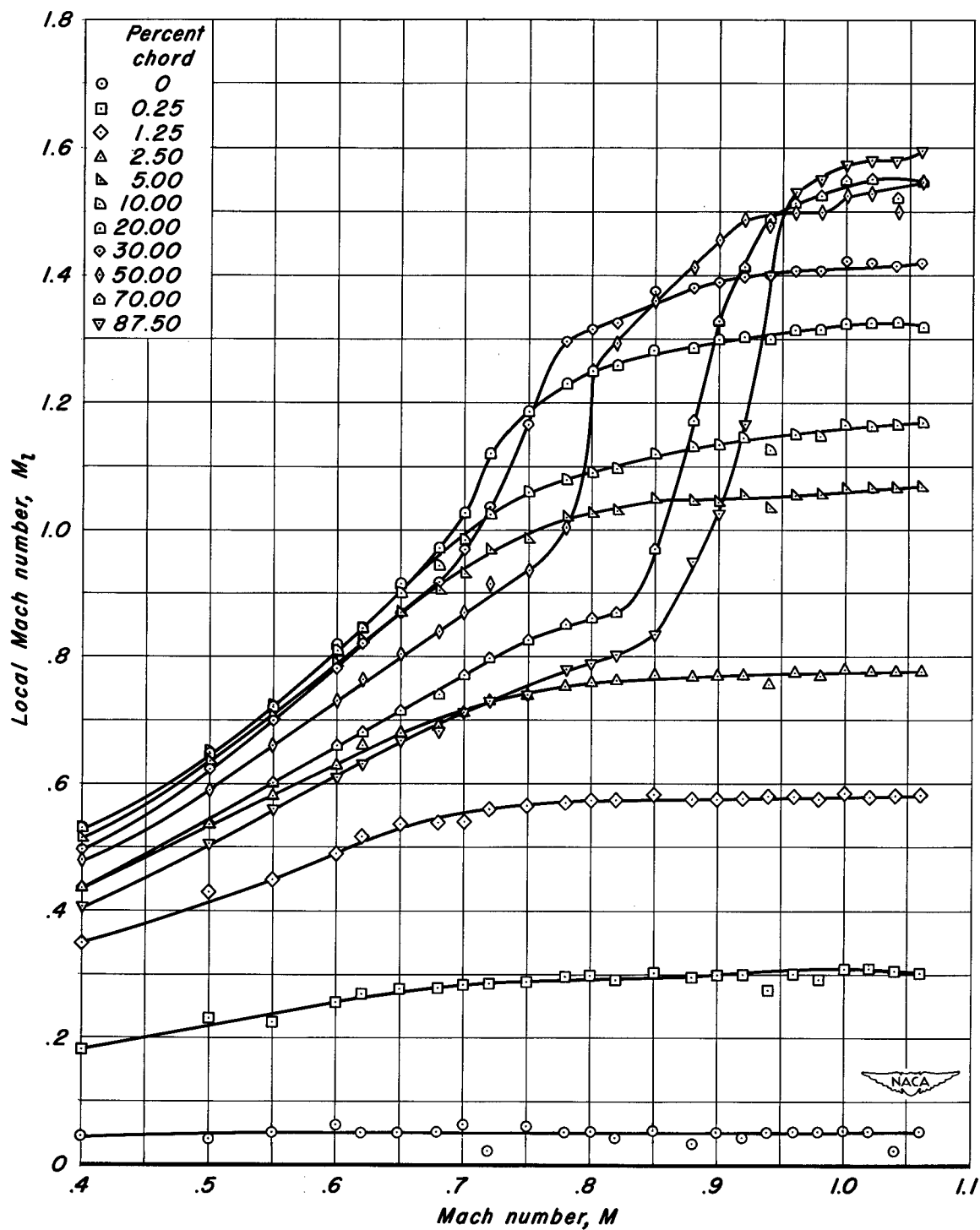
(a) Upper surface.

Figure 8.- Variation of local Mach number with free-stream Mach number at selected chordwise stations for an angle of attack of 0.5° (approximately zero lift).
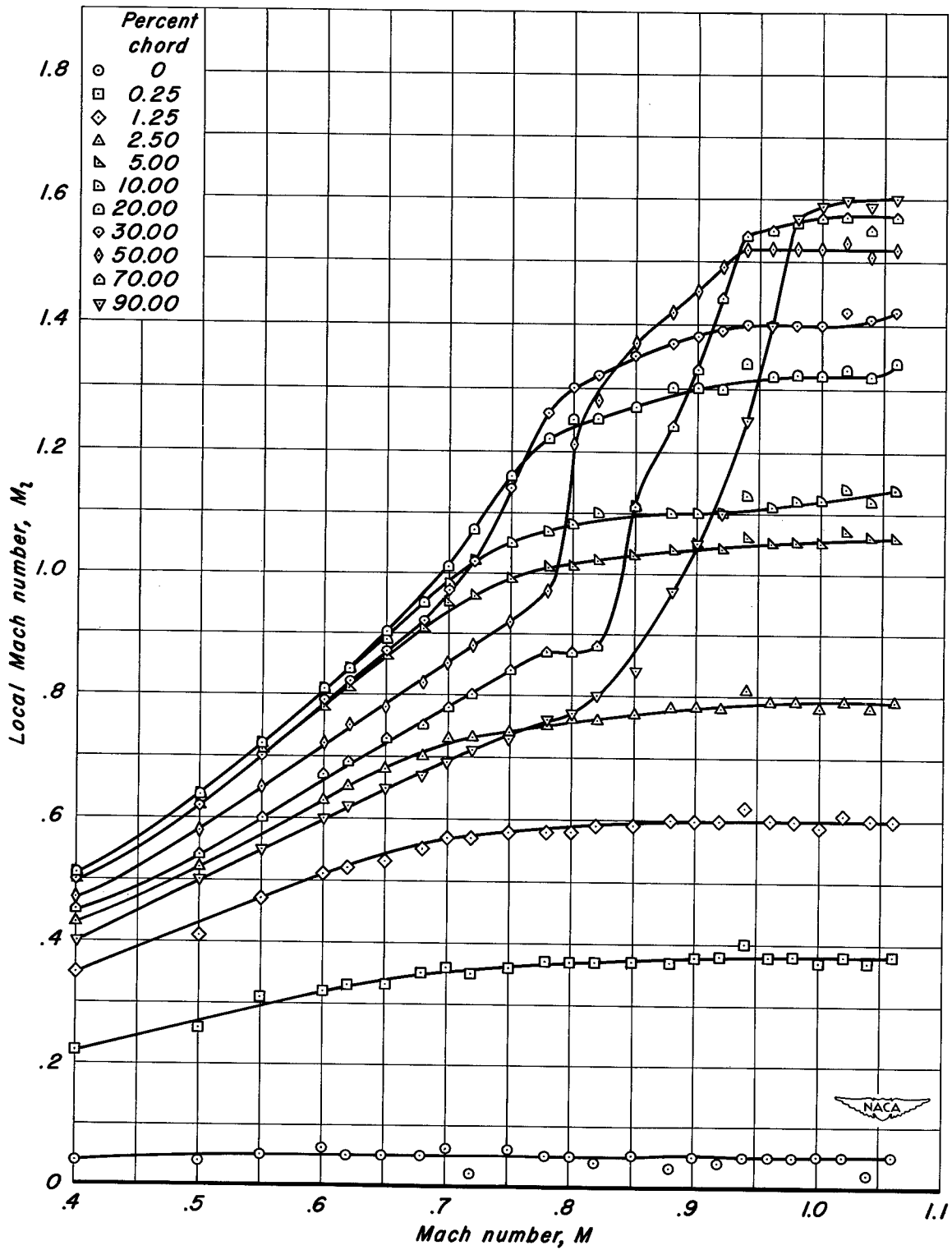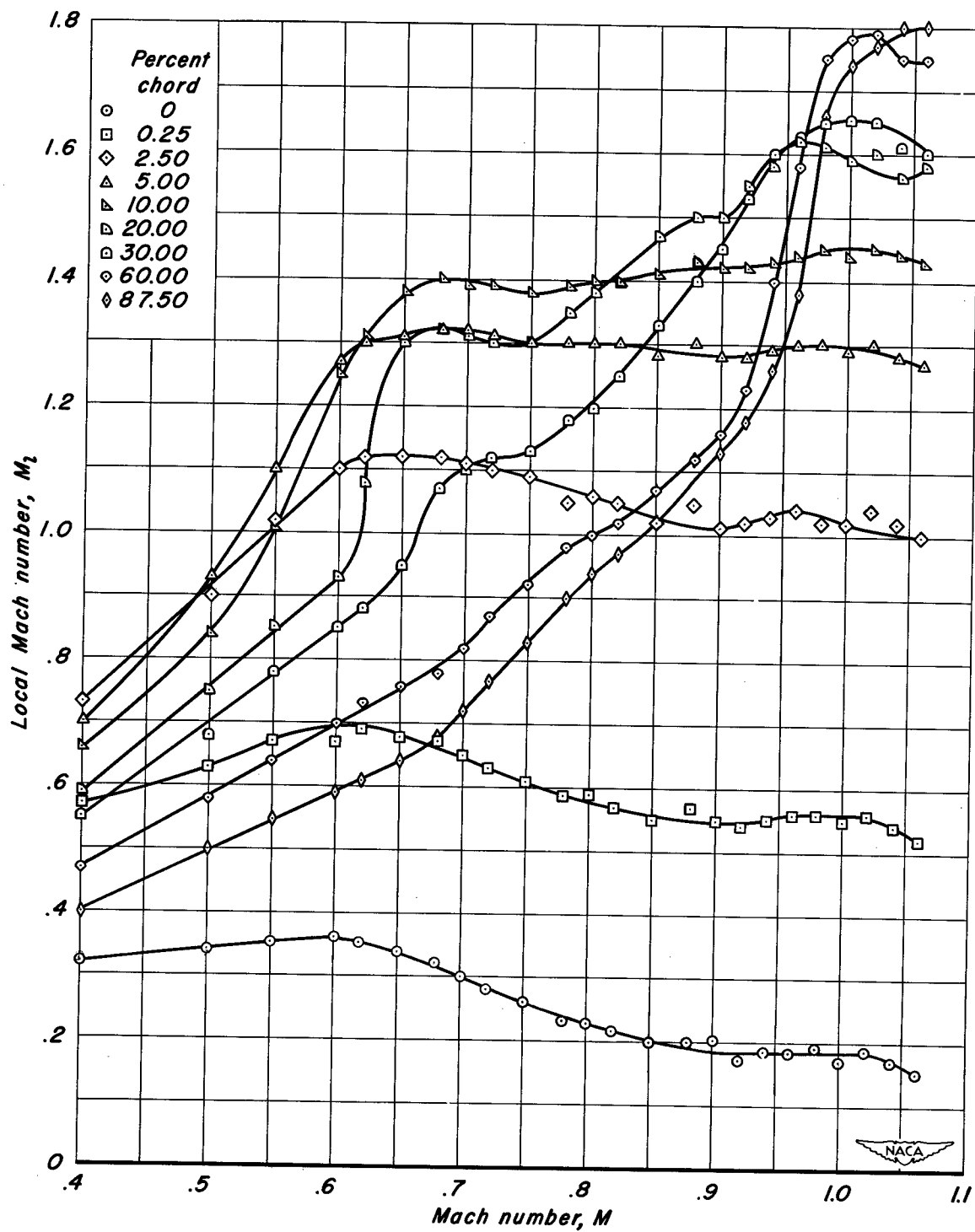
(b) Lower surface.

Figure 8.- Concluded.
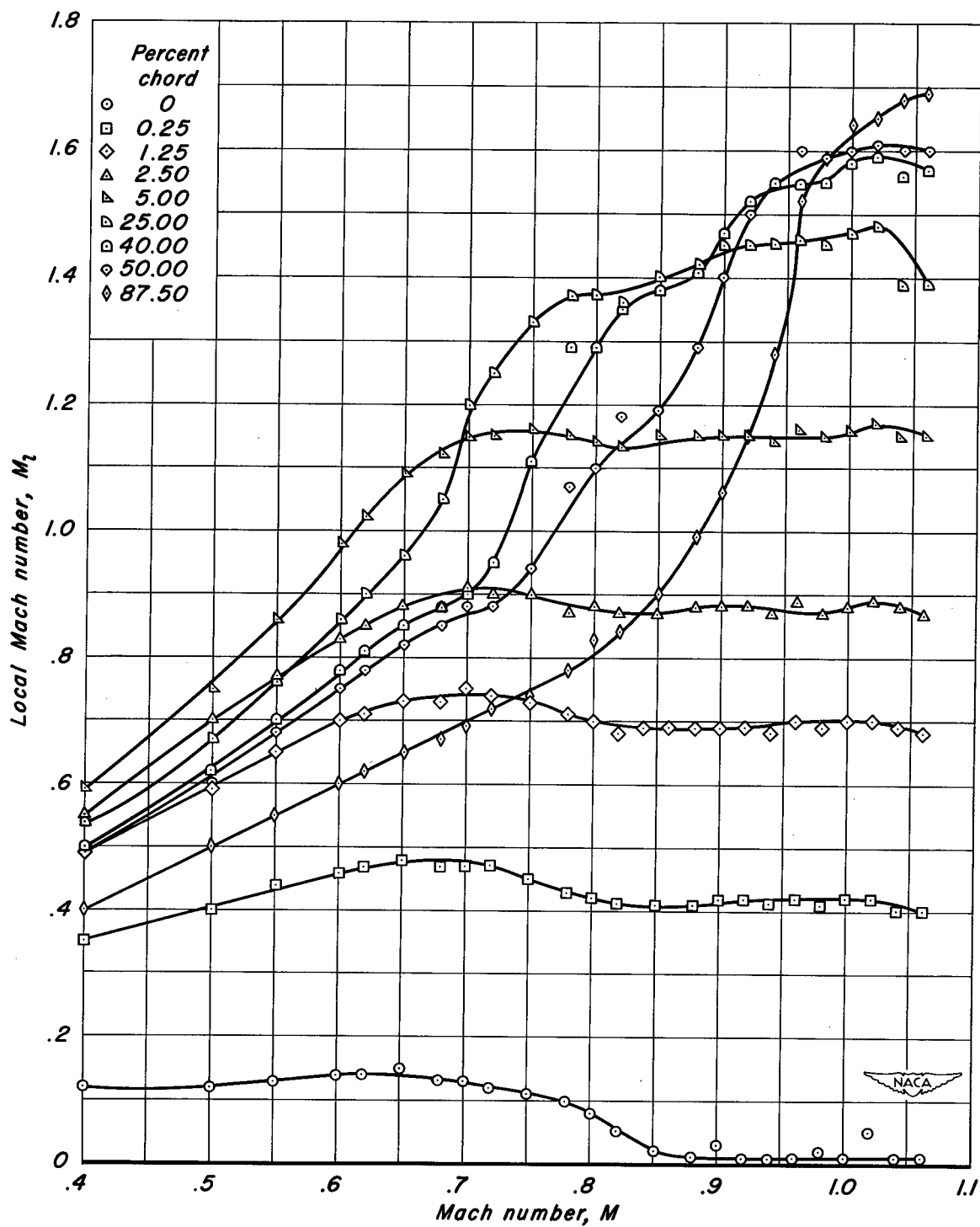
(a) Upper surface.

Figure 9.- Variation of local Mach number with free-stream Mach number
at selected chordwise stations for an angle of attack of 4.0°.
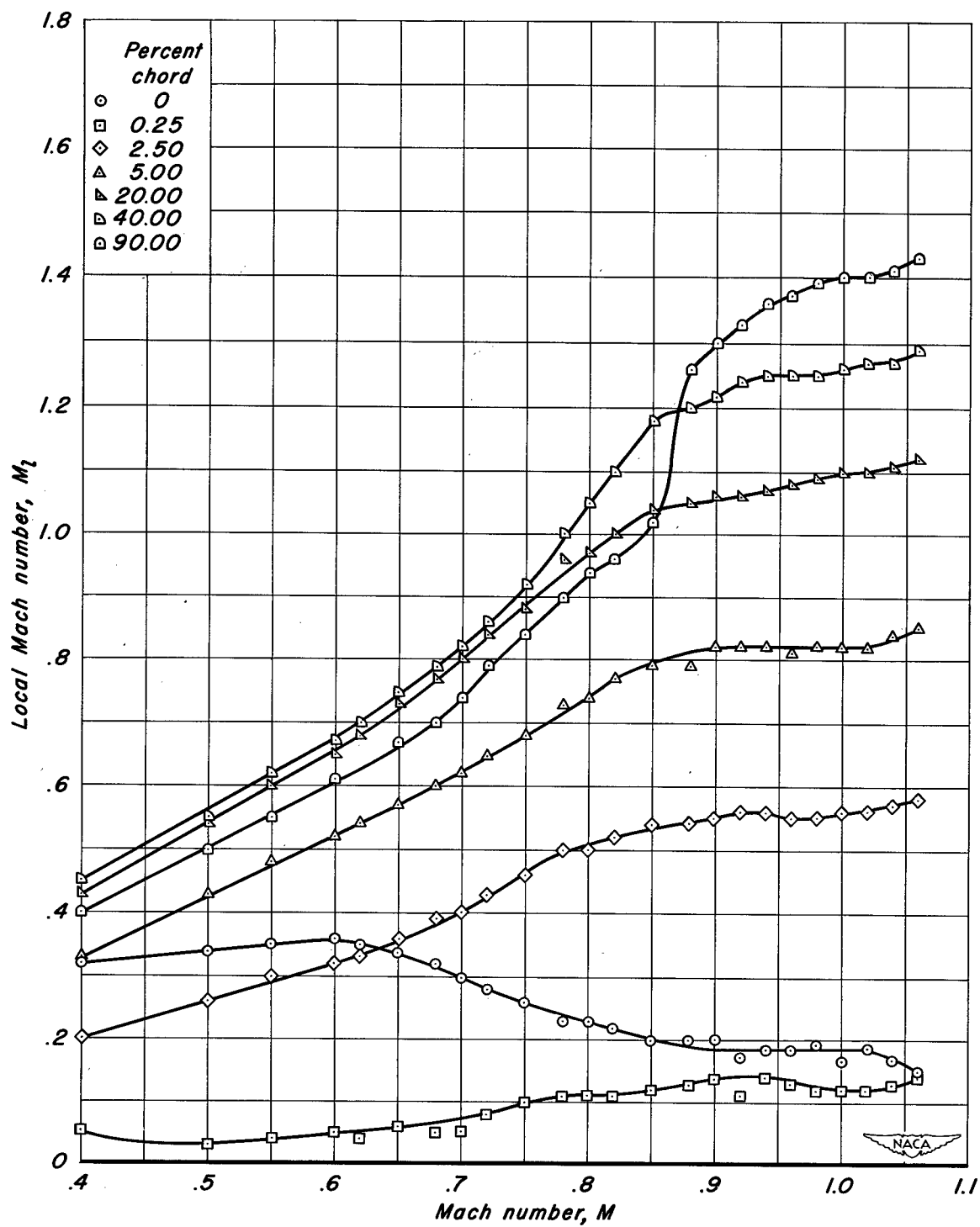
(b) Lower surface.

Figure 9.- Concluded.

(a) Upper surface.

Figure 10.- Variation of local Mach number with free-stream Mach number at selected chordwise stations for an angle of attack of 8.0°.
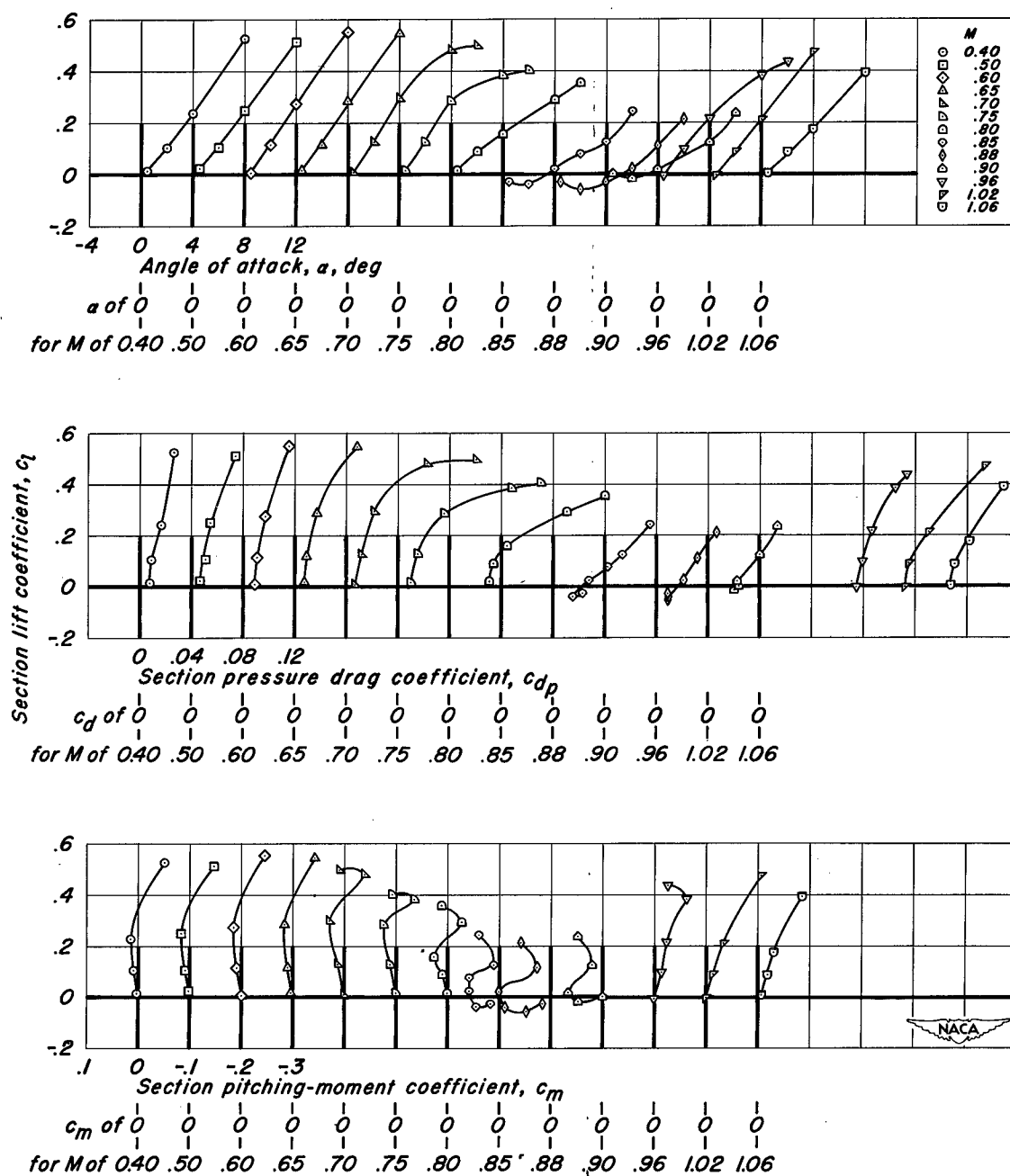
(b) Lower surface.

Figure 10.- Concluded.

Figure 11.- Section lift, pressure drag, and quarter-chord pitching-
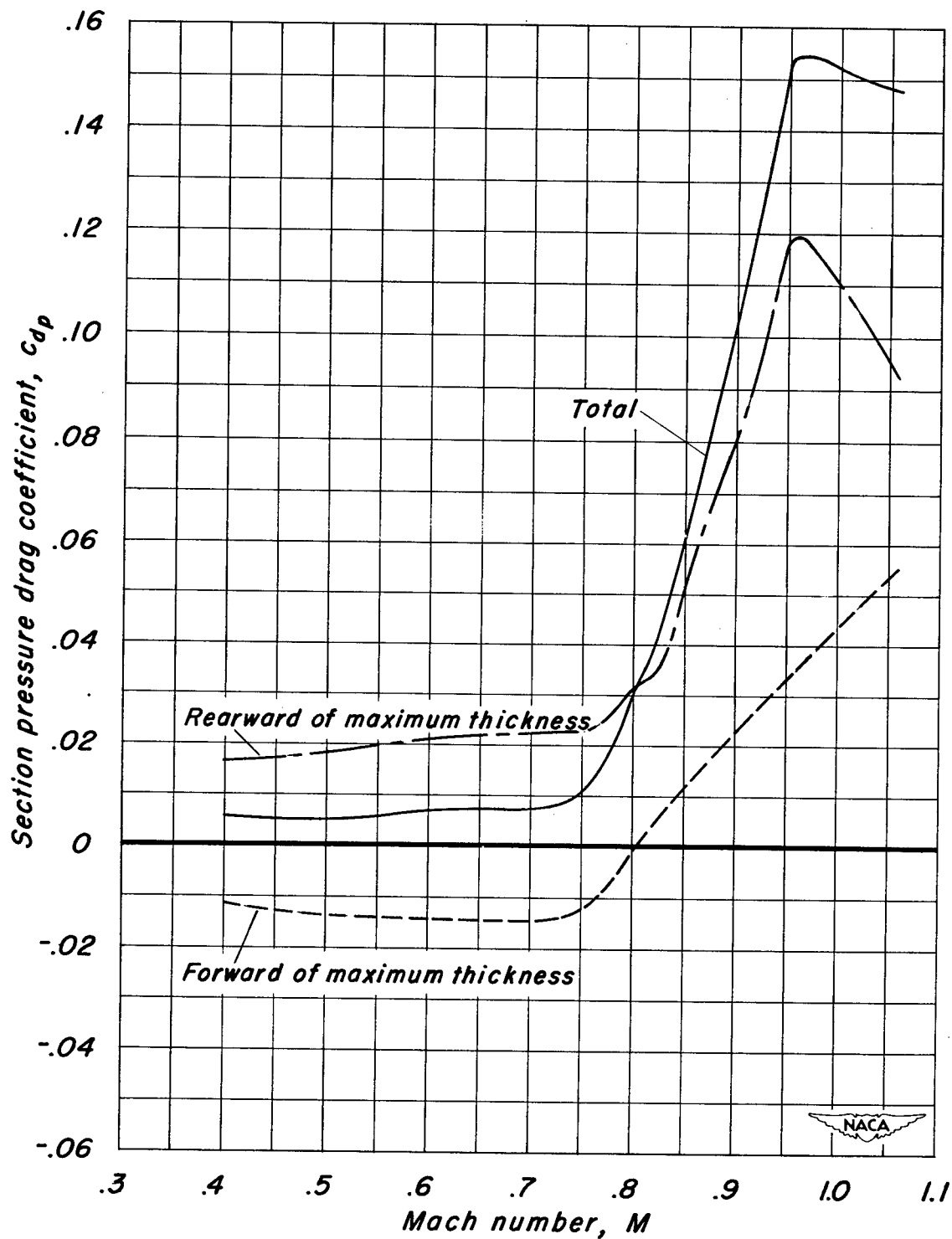moment characteristics.

Figure 12.- The effect of Mach number on that part of the total section pressure drag coefficient due to the components of the airfoil forward and rearward of the point of maximum thickness.